역기전력 추정에 의한 영구자석형 동기 전동기의 토오크 리플의 저감화

조 관열°, 배 정도, 정 세교, 윤 명중
한국과학 기술원, 전기 및 전자공학과

Torque Ripple Minimization in a PM Synchronous Motor with Back EMF Estimation

Kwan-Yuhl Cho, Jung-Do Bae, Se-Kyo Chung, and Myung-Joong Youn
Dept. of Electrical Engineering, KAIST

Abstract

A predictive current control in the synchronous reference frame with the back EMF estimation using the previous voltages and currents is proposed. To reduce the torque ripple produced by harmonics in the air gap flux, the q-axis current is compensated using the estimated torque constant. The effectiveness of the proposed control is compared to the conventional control scheme through the simulation.

I. Introduction

The PM synchronous motor and drives are being used increasingly in a wide range of applications due to their high power density, large torque to inertia ratio, and high efficiency. PM synchronous motors can be classified into two types based on its rotor magnet configuration such as surface permanent magnet(SPM) synchronous motor where magnets are mounted on the rotor surface, and the interior permanent magnet(IPM) synchronous motor where magnets are mounted inside the rotor. The SPM synchronous motor is most commonly used for industrial applications.

The torque-speed characteristics of a PM synchronous motor can be similar to that of a separately excited dc motor employing the vector control(field oriented control). In the vector control of a PM synchronous motor, the torque is controlled by the torque component current(quadrature axis current : i_q) and the field component current(direct axis current : i_d) is controlled to zero below the base speed to maximize the torque to current ratio. To achieve the constant power operation above the base speed, the flux weakening control is performed by the field component current. Since the air-gap flux of a PM synchronous motor is non-sinusoidal, the back EMF in this kind of machine is generally non-sinusoidal due to the magnet shape and the existence of stator slots. The interaction between the back EMF harmonics and sinusoidal current introduces the ripple in the electromagnetic torque. The effect of the torque ripple is worse at low speeds because of its influence on the speed and position control accuracy[1-3]. Since the torque performance is directly influenced by the current control, various current control techniques have been presented[4-8].

In a PM synchronous motor, the torque is proportional to the q-axis current in the synchronous reference frame, therefore, the current control in the synchronous reference frame is preferred to that in the stationary reference frame. In the conventional proportional - integral(PI) plus decoupling current control, the current response is slow and has some overshoots under certain operating points when the fixed gains are used [4-5]. On the other hand, in the predictive control scheme the switching instants of the power switches are determined by calculating the required voltage forcing the motor currents to follow its references. This control scheme provides the constant switching frequency and the lower current ripple, however, the machine parameters and the operating conditions have to be known with sufficient accuracy. The influence of the error in the back EMF on the steady-state response is much more significant than that of the errors in the stator resistance and the inductance[6-8]. In this paper, the back EMFs in the synchronous reference frame are estimated using the previous voltages and the currents so that he current response is independent of the back EMF harmonics and the back EMF variations. In addition, the torque ripple is minimized by compensation of the torque constant using the estimated back EMF.

II. Current Control with Back EMF Estimation

A. Current control with back EMF estimation: In general, a PM synchronous motor has 3 phase stator windings and a permanent magnet rotor. The permeability of a magnet, such as using ND-B-Fe, is effectively that of air($\mu_r = 1.05 \sim 1.2$), therefore, the d-axis inductance is nearly equal to the q-axis inductance. The voltage equation of the PM synchronous motor in the synchronous reference frame can be expressed as follows:

$$v_d = R_s i_d + L_d \frac{d}{dt} i_d - \omega_r L_q i_q + e_d$$

$$v_q = R_s i_q + L_q \frac{d}{dt} i_q + \omega_r L_d i_d + e_q \qquad (1)$$

where R_s is the stator resistance, L_d and L_q are the d-axis and the q-axis inductances, respectively, and ω_r is the electrical angular velocity. Also e_d and e_q are the d-axis and the q-axis back EMFs, respectively, and given by

$$e_d = (E_5 - E_7)\sin 6\theta_r = \omega_r \psi_{d6} \sin 6\theta_r$$

$$e_q = E_1 + (E_5 + E_7)\cos 6\theta_r = \omega_r(\psi_f + \psi_{q6}\cos 6\theta_r) \quad (2)$$

where ψ_f is the flux linkage of a permanent magnet, and E_5 and E_7 are the 5th and 7th order harmonics of the back EMF caused by the non-sinusoidal air gap flux, respectively. The back EMF can be assumed to be constant between the sampling instants because the speed dynamics is slow within a sampling period. The voltage equation in the discrete time domain can be expressed as

$$v_d(k) = R_s i_d(k) + \frac{L_d}{T}(i_d(k+1) - i_d(k)) - L_q \omega_r(k) i_q(k) + e_d(k)$$

$$v_q(k) = R_s i_q(k) + \frac{L_q}{T}(i_q(k+1) - i_q(k)) + L_d \omega_r(k) i_d(k) + e_q(k) \quad (3)$$

where T is a sampling period. The required voltages which make the current errors at $(k+1)$-th sampling instant zero using the estimated back EMFs can be obtained as

$$v_d^*(k) = R_s i_d(k) + \frac{L_d}{T}(i_d^*(k+1) - i_d(k)) - L_q \omega_r(k) i_q(k) + \hat{e}_d(k)$$

$$v_q^*(k) = R_s i_q(k) + \frac{L_q}{T}(i_q^*(k+1) - i_q(k)) + L_d \omega_r(k) i_d(k) + \hat{e}_q(k) \quad (4)$$

where $i_d^*(k+1)$ and $i_q^*(k+1)$ are the d-axis and the q-axis current references at $(k+1)$-th instant, respectively, and $\hat{e}_d(k)$ and $\hat{e}_q(k)$ are the d-axis and the q-axis estimated back EMFs, respectively. It can be noted that the influence of the error in the back EMF on the steady state response is much significant than that in R_s, L_d, and L_q. To obtain the required voltage independent of the back EMFs, the back EMFs are estimated using the previous voltages, previous and present currents, and the rotor speed. Form eqn. 3, $(k-1)$-th back EMF can be obtained as

$$e_d(k-1) = v_d(k-1) - R_s i_d(k-1) - \frac{L_d}{T}(i_d(k) - i_d(k-1)) + L_q \omega_r(k-1) i_q(k-1)$$

$$e_q(k-1) = v_q(k-1) - R_s i_q(k-1) - \frac{L_q}{T}(i_q(k) - i_q(k-1)) - L_d \omega_r(k-1) i_d(k-1). \quad (5)$$

The k-th back EMFs can be obtained from $(k-1)$-th back EMFs using the relations given by the following equations:

$$\hat{e}_d(k) = \frac{\omega_r(k)}{\omega_r(k-1)} e_d(k-1)$$

$$\hat{e}_q(k) = \frac{\omega_r(k)}{\omega_r(k-1)} e_q(k-1). \quad (6)$$

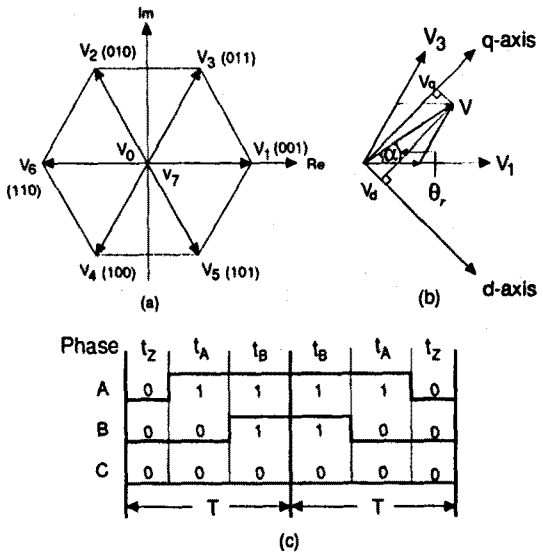

Fig. 1 (a) Inverter voltage space vectors
(b) vector diagram for computation example
(c) switching states.

Table 1 8 operating states for the inverter

state	SC	SB	SA	operating mode	voltage vector
0	0	0	0	free-wheeling	V_0
1	0	0	1	active	V_1
2	0	1	0	active	V_2
3	0	1	1	active	V_3
4	1	0	0	active	V_4
5	1	0	1	active	V_5
6	1	1	0	active	V_6
7	1	1	1	free-wheeling	V_7

B. Voltage control: To obtain the average voltage equal to the required voltage vector $v(k)$, the conduction times of the inverter switches are modulated according to the amplitude and the angle of the voltage vector. Fig. 1(a) shows the inverter voltage space vectors corresponding to the switching states of 3 legs of the inverter, and the 8 operating states for the inverter is shown in Table 1. Since the inverter can take one of the 8 conduction states, V_0 through V_7, the pulsewidth modulation can be used to provide the voltage space vector $v(k)$. In the example shown in Fig. 1(b), the inverter is switched from V_1 to V_3 with the duty cycle determined by the values of v_d and v_q. The time durations of the states 1 and 3, and the zero voltage states are given by

$$\frac{t_A}{T} = \frac{\sqrt{3}\,|v|}{V_{dc}} \sin(60° - \alpha)$$

$$\frac{t_B}{T} = \frac{\sqrt{3}\,|v|}{V_{dc}} \sin\alpha \quad (7)$$

$$t_Z = T - t_A - t_B$$

where V_{dc} is a dc link voltage, and $|v|$ and α are given as follows:

$$|v| = \sqrt{v_d^2 + v_q^2}$$

$$\alpha = \theta_r - \tan^{-1}\left(\frac{v_d}{v_q}\right) \tag{8}$$

where θ_r is the rotor position.

C. Simulation results: The parameters used in the simulation are as follows: R_s = 1[Ω], $L_d = L_q$ = 9[mH], ψ_f = 0.2[Wb], V_{dc} = 240[V], f_s = 50[Hz], and E_5 and E_7 are 3% and 1% of the fundamental component of the back EMF, respectively. The q-axis current reference is 4[A] and changed to 2[A] at 20[msec]. Fig. 2(a) shows the dq currents, a phase current at each sampling instants and these real currents are shown in Fig. 2(b) when the flux linkage of a permanent magnet(ψ_f) is varied 20% high and the back EMF harmonics exist at 10[msec]. Similar waveforms for the current control with back EMF estimation are shown in Fig. 3. In the conventional predictive control, there exist the current offsets due to the inexact back EMFs and the current harmonics of order 6 due to the back EMF harmonics. These current offsets and 6th order harmonics are effectively reduced by the estimation of the back EMF in the proposed control.

III. Torque Ripple Minimization

A. Torque ripple minimization: The electromagnetic torque developed in a PM synchronous motor can be considered as the interaction of the currents in the stator windings and the magnetic field produced by the rotor magnets. This electromagnetic torque can be expressed using the variables in the synchronous reference frame as

$$T_e = \frac{Power}{\omega_r} = \frac{3P}{2}\frac{(e_d i_d + e_q i_q)}{\omega_r} \tag{9}$$

where P is the number of rotor pole pairs. The electromagnetic torque contains an average component and 6th order harmonics. Since i_d is controlled to be zero to maximize the torque to current ratio, the torque depends only on e_q and i_q, and is given by

$$T_e = \frac{3P}{2}(\psi_f + \psi_{q6}\cos 6\theta_r) i_q$$

$$= \frac{3P}{2}\psi_f' i_q. \tag{10}$$

Since ψ_f' has 6th order harmonic, the 6th order torque harmonic exist when i_q is controlled to be constant. However, the torque ripple can be minimized by generating the q-axis current reference i_q^* using the estimated torque constant $\hat{\psi}_f'$. $\hat{\psi}_f'$ and i_q^* are given as follows:

$$\hat{\psi}_f' = \frac{\hat{e}_q(k)}{\omega_r(k)} \tag{11}$$

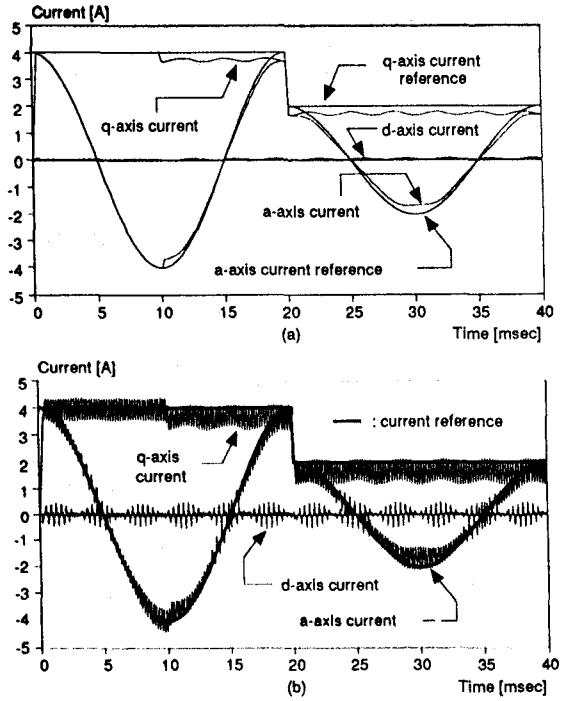

Fig. 2 Predictive current control
(a) dq currents and phase current at sampling instant
(b) real dq currents and phase current.

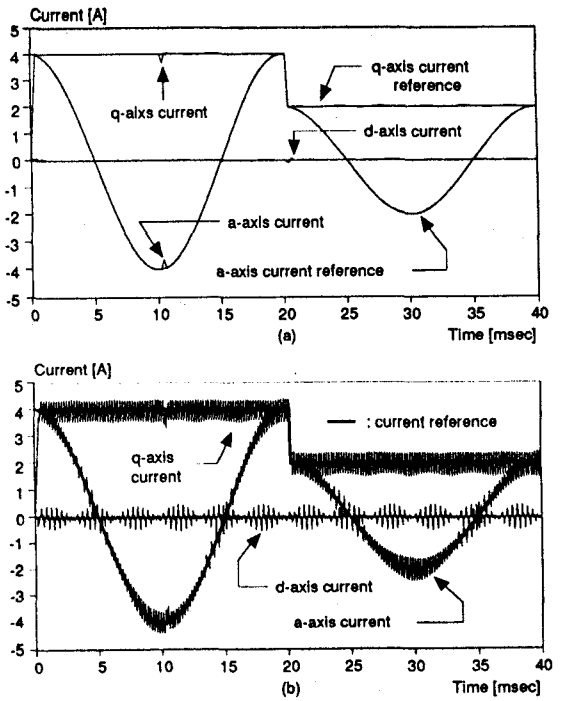

Fig. 3 Proposed current control with back EMF estimation
(a) dq currents and phase current at sampling instant
(b) real dq currents and phase current.

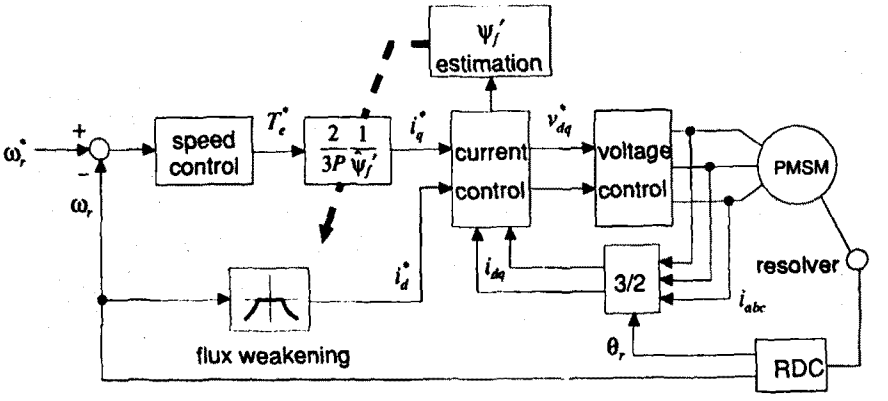

Fig. 4 Overall block diagram of proposed control

$$i_q^* = \frac{T_e^*}{(3P/2)\cdot\hat{\psi}_f'} \tag{12}$$

where T_e^* is the torque command.

B. Control implementation and simulations: Fig. 4 shows the overall block diagram of the proposed torque control using the estimated back EMF to minimize the torque ripple. The torque command is generated by the speed error through the proportional integral(PI) control and produces the q-axis current reference using the estimated torque constant($\hat{\psi}_f'$) to minimize the torque ripple. The measured currents are transformed to the synchronous reference frame and compared to the dq current references. The error is then processed by a predictive current control with the back EMF estimation to provide the voltage reference which makes the current error zero without the information on the back EMFs. Fig. 5 shows the real and estimated back EMFs. The d-axis and the q-axis back EMFs are well estimated with small time delay which can be neglected. The estimation errors can be further reduced by decreasing the sampling period. Fig. 6(a) shows the q-axis current, a phase current, and the generated electromagnetic torque in the conventional scheme with the hysteresis current control. Those for the proposed control are shown in Fig. 6(b). The switching strategy in the hysteresis control is random and the 6th order torque harmonic exists, where the peak value is 15% of the average torque, and this torque ripple is directly reflected to the speed ripple. In the proposed control, the switching strategy is well defined and the 6th order torque ripple is effectively reduced by the compensation of the q-axis current reference using the estimated torque constant.

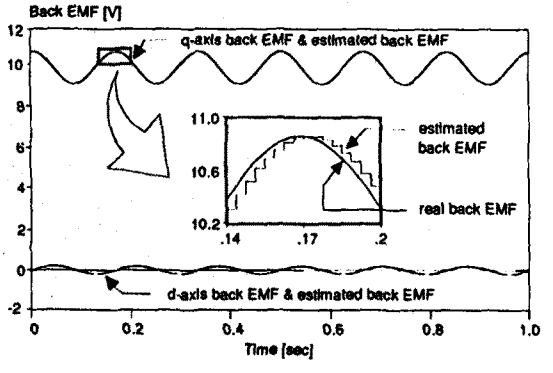

Fig. 5 Real and estimated back EMFs

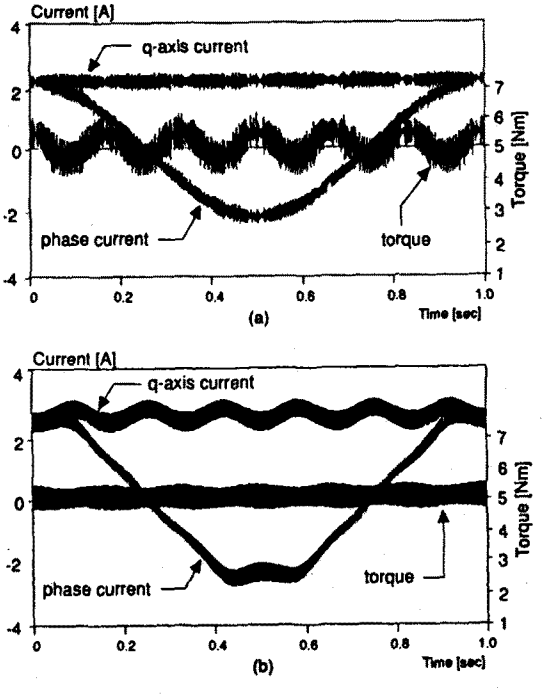

Fig. 6 Q-axis, a-axis current, and electromagnetic torque
(a) conventional scheme with hysteresis current control
(b) proposed control with torque constant compensation

IV. Conclusion

The predictive current control in the synchronous reference frame using the back EMF estimation is proposed, where this control is independent of the back EMF variations and harmonics. To reduce the torque ripple at low speeds, the q-axis current reference is compensated by the torque constant estimated in the current controller. It is verified that back EMF is well estimated and the torque ripple is effectively reduced.

References

[1] R. Carlson, A. A. Tavares, J. P. Bastos, and M. L. Mazenc," Torque ripple attenuation in permanent magnet synchronous motors," Conf. Rec. of IEEE - IAS Annual Meeting, San Diego, pp. 57-62, 1989

[2] BH Ng, MF Rahmant, TS Low, and KW Lim," An investigation into the effect of machine parameters on torque pulsations in brushless dc drive," Conf. Rec. of IEEE - IECON, Philadelphia, pp. 749-754, 1989

[3] L. Norum, A. K. Adnanes, W. Sulkowski, L. A. Aga," The realization of a permanent magnet synchronous motor drive with digital voltage vector selection current controller," Conf. Rec. of IEEE - IECON, Kobe, pp. 182-187, 1991

[4] T. M. Rowan and R. J. Kerkman," A new synchronous current regulator and analysis of current-regulated PWM inverters," IEEE Trans. Ind. Appl., vol. 22, no. 4, pp. 678-690, 1986

[5] H. L. Huy and L. A. Dessaint," An adaptive current control scheme for PWM synchronous motor drives : analysis and simulation," IEEE Trans. Power Elect., vol. 4, no. 4, pp. 486-495, 1989

[6] N. Matsui and H. Ohashi," DSP-based adaptive control of a brushless motor," IEEE Trans. on Ind. Appl., vol. 28, no. 2, pp. 448-454, 1992

[7] T. S. Low, T. H. Lee, K. J. Tseng, and K. S. Lock," Servo performance of a BLDC drive with instantaneous torque control," IEEE on Trans. Ind. Appl., vol. 28, no. 2, pp. 455-462, 1992

[8] D. S. Oh, K. Y. Cho, and M. J. Youn," A discretized current control technique with delayed input voltage feedback for a voltage-fed PWM inverter," IEEE Trans. on Power Elect., vol. 7, no. 2, pp. 364-373, 1992